Journal of
MATERIALS RESEARCH

Phase structure and thermal evolution in coating films and powders obtained by sol-gel process: Part II. ZrO_2–2.5 mole % Y_2O_3

R. Caruso, E. Benavídez, and O. de Sanctis
Laboratorio de Materiales Cerámicos, FCEIyA, IFIR, Av. Pellegrini 250, 2000 Rosario, Argentina

M. C. Caracoche and P. C. Rivas
Programa TENAES, Departamento de Física, FCE, Universidad Nacional de La Plata, c.c. 67, 1900 La Plata, Argentina

M. Cervera
Departamento de Ciencia y Tecnología, Universidad Nacional de Quilmes, R.S. 184, 1864 Bernal, Argentina

A. Caneiro and A. Serquis
Centro Atómico Bariloche, CNEA, 8400 Bariloche, Argentina

(Received 4 September 1996; accepted 16 June 1997)

Powders and coatings of zirconia doped with 2.5 mole % yttria have been produced via the sol-gel route. The phase structure and subsequent thermal evolution in heating and cooling cycles have been investigated using mainly perturbed angular correlations spectroscopy. Thermal analyses and XRD as a function of temperature have also been performed to obtain complementary information. Upon heating, the amorphous gels crystallized into the tetragonal structure and showed the same hyperfine pattern and thermal behavior as observed in tetragonal zirconia obtained by the ceramic route: the two configurations of vacancies around zirconium ions denoted as t_1 and t_2 forms and their mutual $t_1 \rightarrow t_2$ transformation. While the powder sample exhibited an incipient thermal instability above 1000 °C and underwent completely the t_2 form to m–ZrO_2 transition during subsequent, gradual cooling below 500 °C, the coating retained the tetragonal phase within the whole temperature range investigated. Hyperfine results suggest that the tetragonal phase stabilization is favored by the highly defective nature of the t_1 form and consequently hardened by the availability of oxygen. The PAC derived activation energy for the fast diffusion of the oxygen vacancies inherent to the t_2 form was determined as 0.54 ± 0.14 eV.

I. INTRODUCTION

Among the advanced ceramics, yttria stabilized cubic and tetragonal zirconias have exhibited improved mechanical and electrical properties.[1] The tetragonal phase, in particular, which is believed to be responsible for the enhanced toughness, has received much attention concerning its stabilization and retention under various working conditions.[2]

It is already known that the sol-gel route allows the synthesis of nanocrystalline particulates and subsequent densification with retained fine grain size.[3] As this situation favors the crystallization of zirconia metastable phases,[4] the method constitutes an efficient means to obtain ZrO_2-based stabilized ceramics. This chemical method involves a molecular precursor metal alkoxide as $Zr(OR)_n$ which, via inorganic polycondensation reactions, results in a hydroxide or oxide network. The size of the particle depends on the relative rates of the hydrolysis and condensation reactions, which are in turn determined by externally controllable parameters during the synthesis.[5,6]

The present study is part of a research line on sol-gel derived base-ZrO_2 ceramic powders and coatings using a zirconium alkoxide as starting material. Results of previous investigations[6–8] involving pure and yttria-doped cubic zirconias obtained by Perturbed Angular Correlations (PAC) spectroscopy have encouraged the authors to continue with the project, the aim being to produce tetragonal powders and coatings of ZrO_2–2.5 mole % Y_2O_3 composition and to apply the same hyperfine technique to investigate the local environments of zirconium cations and the thermal stability and electrical properties of these ceramic materials. Experimental results have been complemented with XRD data and thermal analyses.

The PAC method is a nuclear technique by which the hyperfine interaction between a radioactive nucleus acting as a probe and the internal fields of the solid

in the nearest neighborhood can be measured.[8–10] If the nuclear properties of the probe are known, the method provides knowledge of the electric field gradient (EFG) and/or the magnetic field characteristic of the crystalline lattice, via the determination of their typical PAC parameters. The technique has proved quite efficient for investigating the quadrupole hyperfine interaction in zirconium-containing materials since the naturally occurring hafnium impurities in zirconium, upon neutron irradiation, lead to the well-known ^{181}Hf probe nuclei. These decay by emission to an excited state of ^{181}Ta and by emission of two gamma rays in cascade ($\gamma_1 = 133$ keV and $\gamma_2 = 482$ keV) to the ground state of ^{181}Ta. The well-established anisotropy in the directions of emission between the first and the second photons of the gamma-gamma cascade is described by the correlation function $W(\theta, t)$ or probability per unit time that γ_2 be emitted at an angle θ and delayed a time t with respect to the direction and time of emission of γ_1. If the intermediate nuclear state in the cascade presents a mean lifetime that is long enough, the nuclei will be reoriented due to the hyperfine interaction between the nucleus and the internal fields around them and the angular correlation will become perturbed. The effect, reflected in the $R(t)$ function or spin rotation curve drawn in a PAC experiment, gives the desired information about the EFG via the determination of the four quantities, i.e., relative fraction, quadrupole frequency, asymmetry parameter, and frequency spread ($f, \omega_Q, \eta, \delta$), associated with each unequivalent zirconium lattice site.[8] This determination is carried out through a computational fitting procedure. The EFG's of monoclinic and tetragonal equilibrium phases of zirconia are accurately known.[11]

If measurements are carried out with temperature changes, the technique can be used to study the thermally activated movement of the oxygen vacancies introduced for charge compensation due to the addition of Y_2O_3 to ZrO_2 and/or of other vacancies arising during the gel-oxide conversion. In fact, atomic or defect movements cause a further perturbation of the angular correlation which may be reflected in the PAC spin rotation curves by a damping in the amplitude obeying to a factor of the form $e^{-\lambda t}$ where λ is called the relaxation constant.[12,13] In stabilized zirconias, this situation appears with the onset of the thermally activated vacancy-hopping process. The jump frequency, v obeys an Arrhenius law and the correlation time $\tau = 1/v$ can then be associated with the activation energy of the jump through the equation:

$$\tau_c = \tau_{c\infty} e^{E_{act}/kT}. \quad (1)$$

It has already been reported that an exponential decrease of the relaxation constant with the reciprocal absolute temperature implies a slow diffusion movement for which the correlation time between two successive atomic configurations is equal to λ^{-1}.[14] By contrast, an exponential increase of λ with the reciprocal absolute temperature, generally found at higher temperatures, is typical of a fast relaxation regime, for which the correlation time is proportional to λ.[12,13] Hence, considering Eq. (1), the activation energies for movement of the vacancies can be drawn from the slopes of the λ (T^{-1}) function.

Some PAC investigations have already been performed on tetragonal zirconia-yttria systems in concentrations similar to the present one. Jaeger *et al.*[11] carried out a study on some of these systems prepared via the ceramic route, including one with 2.2 mole% yttria. At high temperatures they found PAC spectra similar to those of pure tetragonal zirconia but exhibiting a considerably greater frequency broadening; at temperatures lower than 700 °C the spectra could not be resolved adequately. Recent results obtained by the present authors[13] on a commercial 2.8 mole% Y_2O_3-tetragonal zirconia indicate that the metastable tetragonal structure exhibits two zirconium surroundings other than the eightfold oxygen coordinated characterizing the equilibrium high temperature t–ZrO_2 tetragonal phase. They were named t_1 and t_2 forms and describe two configurations of oxygen vacancies around zirconium ions, between which a reversible transformation takes place as temperature increases. The less distorted tetragonal t_2 form, involving more distant vacancies, is depicted by a dynamic hyperfine interaction associated with an activation energy of 0.50 ± 0.04 eV for the fast oxygen vacancies movement.

II. EXPERIMENTAL

A. Sample preparation

The starting solution was prepared by stirring zirconium *n*-propoxide (ZNP) (70 wt.% in isopropanol, Alfa 22989), ethanol, and HNO_3 as a catalytic agent in an anhydrous nitrogen atmosphere to avoid hydroxide precipitation. After 6 h, distilled water and acetic acid (3 : 1 wt. ratio) were carefully added, followed by stirring for 24 h until a quite transparent solution was obtained. The $ZNP/H_2O/HNO_3$ molar ratios achieved the 1/7/1 values and the ZrO_2 concentration in the solution was 94.1 g/l. The final sol-gel solution was obtained by adding yttrium acetate (99.9%, Aldrich) dissolved in isopropanol and nitric acid in the zirconium solution. This step was performed under stirring in normal atmosphere. The resulting alcohol/ZNP ratio, H_2O/ZNP ratio, and nominal yttria concentration were determined as 16.6, 7, and 2.5 mole%, respectively.

Tubes of 2 cm height and 0.5 cm diameter and small sheets of alumina were used as substrates for the coatings. The liquid films were deposited by dip-coating the substrates into the precursor solution in air atmos-

phere. The withdrawal rate was 8 cm/min. The thickness of the densified monolayer coatings was measured with a Hommel Tester T2 profilometer as 110 nm. Finally, coatings about 1 μm thick were produced by a multilayer deposition process. After each deposition, the film was heated at 500 °C for 1 h to avoid cracking. The powders were prepared by gelating the solutions in an open flask at 60 °C and drying the gels at 120 °C.

B. Thermal analyses and XRD

Differential thermal analysis (DTA) and thermogravimetry analysis (TGA) were carried out on approximately 50 mg of the as-obtained powder in normal atmosphere, at heating and cooling rates of 10 °C/min over the RT-1350 °C range by means of a Netzsche STA 409 analyzer. Moreover, thermogravimetric analyses were performed in ultrapure oxygen and argon atmospheres (negligible water content of less than 3 ppm in both) up to 1060 °C at the same heating rate and 1 atm pressure, using equipment built on the basis of a Cahan 1000 electrobalance specially designed to determine weight changes within ±10 μg under controlled atmosphere.[15]

Powder x-ray diffraction (XRD) data were collected on a Phillips PW1700 diffractometer using Cu K_α radiation and a graphite monochromator (the step size being $2\theta = 0.02°$ with a 5 s time per step). Room temperature XRD data were taken on the as-obtained powder and also in oxygen and argon atmospheres after the corresponding TGA analyses up to 1060 °C had been performed. High temperature XRD patterns were obtained in air atmosphere making use of an Anton–Paar HTK10 high temperature chamber at 200, 400, 600, 800, 1000, and 1200 °C. Glazing angle patterns of the coatings deposited on alumina sheets, as-obtained and heated at 800 °C, were obtained at RT by using a Phillips PW 3710 Diffractometer with a step size of $2\theta = 0.02°$ and a scanning rate of 1 s per step.

XRD spectra of the samples were obtained in the $2\theta = 20°–105°$ diffraction region. The low-angle portion $2\theta = 27°–32°$, at which the most intense peaks of all zirconia polymorphs appear, and the high-angle region $2\theta = 72°–76°$, which allows a decision between tetragonal and cubic zirconia structures, were carefully inspected. Powder diffraction spectra were used to calculate average crystallite sizes from the magnitude of the half-width of the (111) peak by using the Scherrer equation.[16]

C. PAC experiment

The hyperfine interaction was determined using two CsF detectors of temporal resolution $\tau_R = 0.75$ ns. The powder was encapsulated in air at atmospheric pressure, in a 0.5 cm^3 sealed quartz tube. This tube and the zirconia deposited alumina tube were then neutron irradiated with a flux of 10^{13} neutrons cm^{-2} s^{-1} for approximately 1 day to produce suitable hafnium activities of about 100 μCi. One or two day long spectra were obtained for the powder at increasing temperatures up to 1200 °C, with a RT measurement between 1000 and 1100 °C, and then at gradually decreasing temperatures from 1000 °C to RT. The film was measured at gradually increasing temperatures up to 1150 °C. Due to the rather weak radioactivity, only one final experiment, at RT, could be performed on cooling. The mean temperature uncertainty was ±5 °C.

III. RESULTS AND DISCUSSION

The TGA analyses in air showed a behavior similar to that determined under oxygen atmosphere. Figure 1 displays the thermogravimetric results obtained in (a) oxygen and (b) argon atmospheres. Both indicate a continuous mass loss below 550 °C, which is very drastic up to 360 °C. While the largest mass loss is known to be related to the successive elimination of adsorbed solvent and water, bound water, and organic residues,[6] the gradual weight loss above 360 °C has been reported to reflect the removal of surface hydroxyls.[17] The two experiments give similar information up to about 450 °C

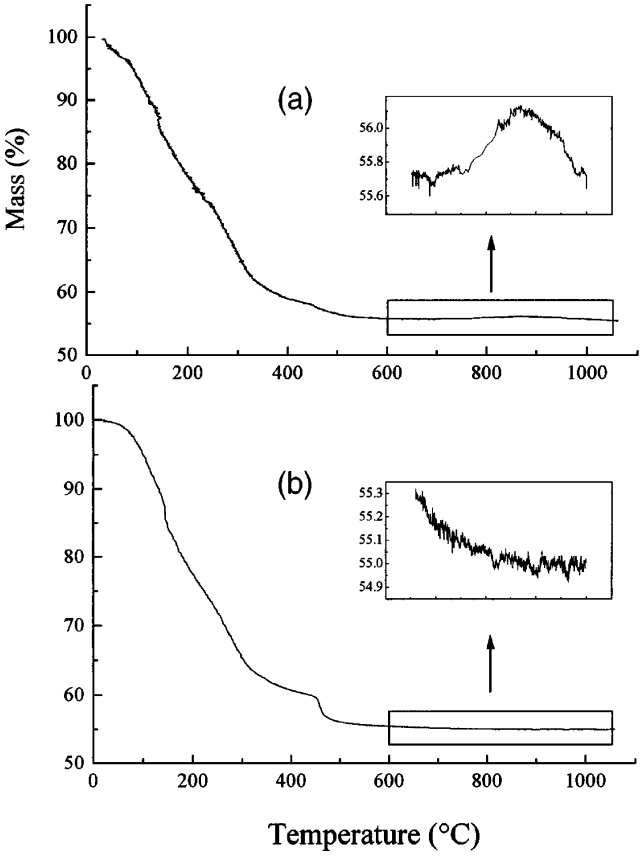

FIG. 1. TGA analyses performed on the ceramic powder in (a) oxygen and (b) argon atmospheres.

and the total mass loss is about 45%. Nevertheless, some differences appear at higher temperatures. The Ar-treated powder plot reveals an abrupt step between 460 and 470 °C and no significant mass change at higher temperatures. The O_2-treated powder, on the other hand, exhibits a smoother mass loss near 450 °C and a small mass gain over 700 °C which we assign to oxygen absorption. The cooling curves show no detectable changes. XRD spectra obtained at RT in oxygen and argon atmospheres just after the corresponding TGA runs up to 1060 °C (see Fig. 2) reveal the presence of only the tetragonal phase in the Ar-treated powder and of tetragonal and monoclinic reflections in the O_2-treated powder. From the calculated average crystallite size appearing at the right of the diffractograms, it can be seen that the heating induced growth of crystallites in oxygen. Figure 3 shows the DTA heating and cooling curves obtained for the powder in normal atmosphere. Though no signals could be resolved in the low temperature region, two neat exothermic peaks at 350 and 450 °C and also a very broad signal centered at 770 °C, known to correspond, respectively, to the elimination of organic groups, the crystallization of amorphous zirconia, and the elimination of the last $(OH)^-$ groups,[8,18] were clearly observed. According to the TGA information, on the other hand, the last DTA change could also be partially

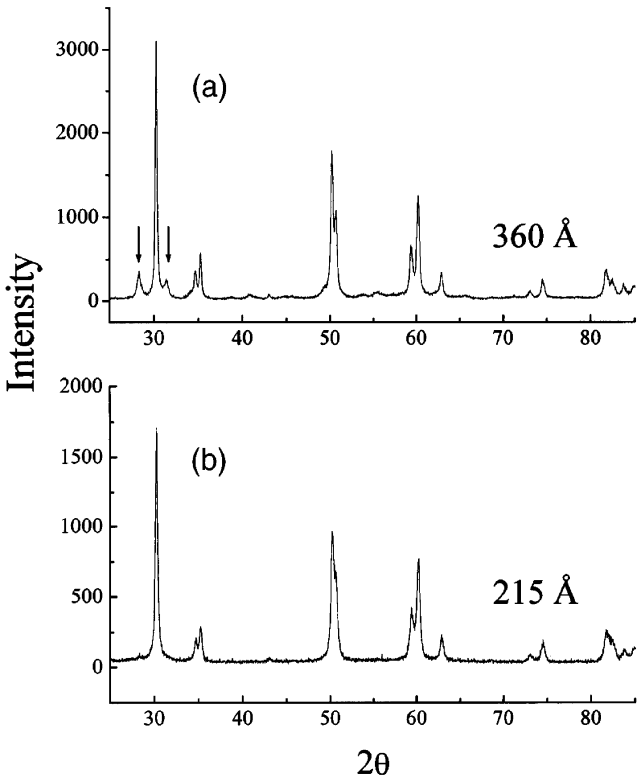

FIG. 2. RT diffraction patterns of the powder obtained after gradual heating up to 1300 °C in (a) oxygen and (b) argon. Arrows indicate the main lines of $m-ZrO_2$. Numbers at the right are calculated average crystallite sizes of the tetragonal phase.

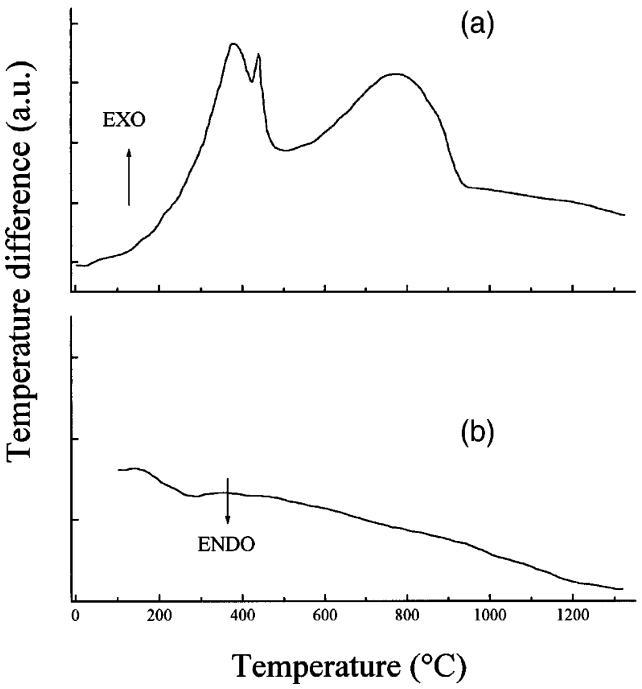

FIG. 3. DTA curves obtained for the $ZrO_2-2.5Y_2O_3$ powder in (a) heating and (b) cooling regimes, in air at 10 °C/min.

associated with the reported oxygen absorption. On cooling, a very weak endothermic signal and rather extensive change appeared below 350 °C.

XRD of the as-obtained powder and coating exhibited, respectively, an amorphous pattern and that typical of tetragonal zirconia. High temperature XRD patterns of the powder shown in Fig. 4 revealed the crystallization of the metastable tetragonal phase above 400 °C and also that this phase remained stable within the whole heating thermal range investigated. Calculated values of the average crystallite size achieved at each temperature, shown at the right of the diffractograms, reveal that significant increases have taken place at 1000 °C and also at 1200 °C.

PAC results are shown in Figs. 5 to 8. In Fig. 5, selected spin rotation curves taken on the powder and the coating during the heating and cooling cycles are plotted. The full lines are the best fits obtained, from which the quadrupole parameters depicting the existing microstructures could be derived. As an example, the powder second spectrum shows the hyperfine components of the contributors to the PAC pattern. Figures 6 and 7 show the thermal evolution of the relative fractions and quadrupole parameters of the hyperfine interactions for both samples during the PAC experiments. The temperature scale indicates, at the same time, the temporal sequence at which measurements were carried out.

In the following paragraphs, experimental evidence drawn for the zirconia powder from the PAC technique, revealed as nanoscopic characteristics, is presented to-

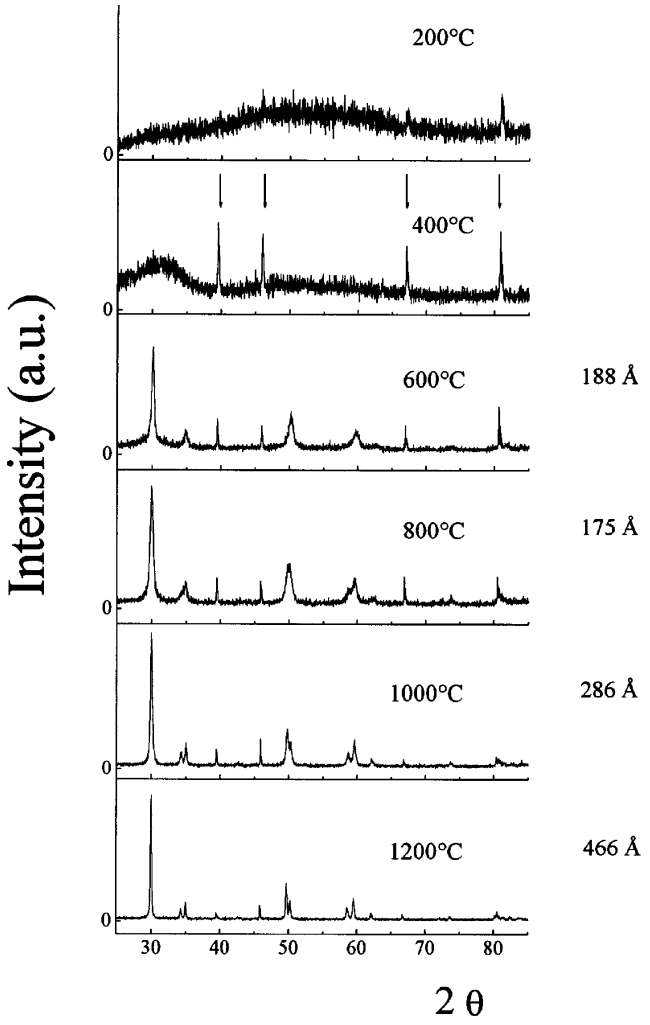

FIG. 4. High temperature XRD patterns of the stabilized zirconia powder. Arrows indicate the diffraction lines corresponding to the platinum substrate. Numbers at the right are calculated average crystallite sizes.

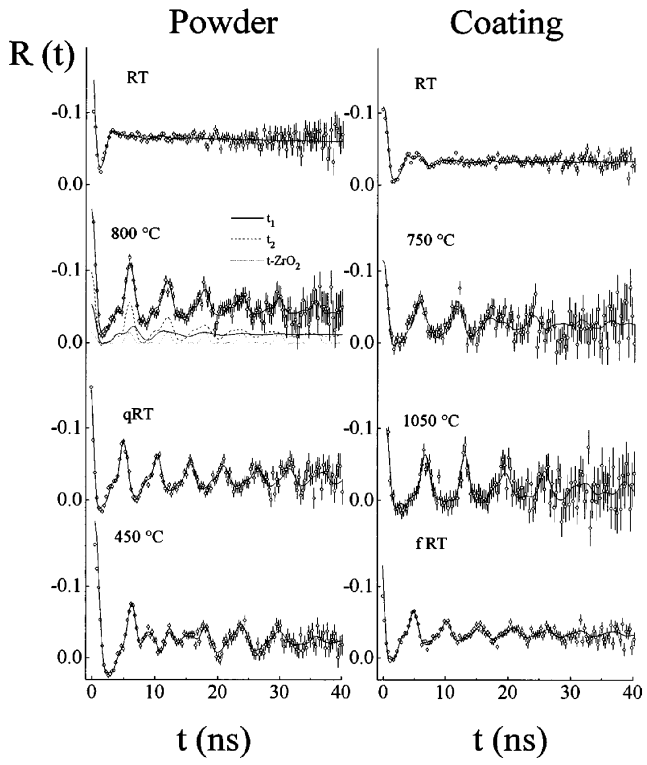

FIG. 5. Spin rotation curves for the powder and the coating at selected temperatures. Full lines are the best fitting curves. qRT denotes the RT powder spectrum obtained between 1000 °C and 1100 °C and fRT denotes the final RT spectrum obtained for the film.

gether with evidence revealed as bulk properties by the other techniques and, when possible, an explanation of the underlying phenomena.

(a) Within the RT–300 °C thermal range, not shown in Fig. 6, two extremely distributed hyperfine interactions already reported in previous works[6,7] depict the very disordered zirconium surroundings of the amorphous zirconia powder which suffers a continuous mass loss.

(b) Though a detailed and thorough investigation of this low temperature region is still lacking, the disappearance at 350 °C of the initially most abundant interaction along with the $(OR)^-$ removal DTA peak and the end of the drastic mass loss observed by TGA allows the assignment of the vanishing interaction to zirconium surroundings involving organic groups. The other interaction, associated in turn with the presence of remaining synthesis derived oxo- and aquo-groups around Zr^{4+} ions, is the same as that reported recently[13] as the metastable tetragonal t_1 form. Hence, it has been identified with a very distorted tetragonal structure containing near, bounded oxygen vacancies within the zirconium neighborhoods. Near 400 °C, the other metastable tetragonal configuration, the already known t_2 form believed to describe zirconium sites involving more distant vacancies, appears. The damping of the spin rotation curve observed from 350 °C on could be satisfactorily fitted only when assigning the dynamic factor $e^{-\lambda t}$ to the interaction describing this last defect configuration. However, though the high frequency spread (at low temperatures) and the small relative fraction (at high temperatures) determined for the t_1 form constituted a technical restriction to fit the movement of the vacancies around these zirconium sites, this possibility must not be discarded. Between 350 and 650 °C the lattice is depicted exclusively by the hyperfine interactions corresponding to the t_1 and t_2 forms. While the first of them exhibits some variations in its η and δ parameters, the thermal behavior of the relaxation constant involved in the dynamic interaction corresponds to a slow diffusion.

(c) Above 450 °C, the decrease of the δ parameter of the most abundant interaction reflects a gradual ordering of the crystalline lattice. This process, also revealed

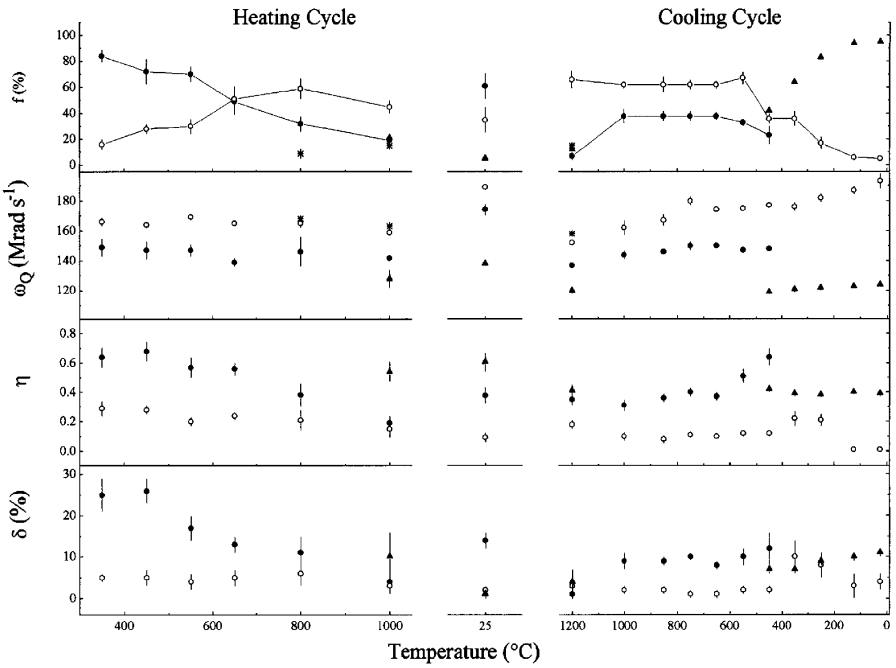

FIG. 6. Thermal evolution of the relative fractions and quadrupole parameters of the hyperfine interactions found for the powder. (●) t_1 form, (○) t_2 form, (★) t–ZrO_2, and (▲) m–ZrO_2. Full lines are to guide the eye. The asymmetry parameter and the distribution width for the equilibrium t–ZrO_2 phase have been set equal to zero and are not represented.

by the high temperature XRD patterns above 400 °C (see Fig. 4), confirms that the second exothermic DTA peak corresponds to the crystallization of amorphous zirconia into the tetragonal polymorph. This evidence leads to the conclusion that crystalline metastable tetragonal zirconia, with a diffraction pattern identical to that of the equilibrium phase, is described at nanoscopic level by two configurations around zirconium ions that are different from those typical of t–ZrO_2.[9]

(d) The triggering of the $t_1 \rightarrow t_2$ transformation observed at 450 °C is followed at 550 °C by a small reduction of the η parameter of the t_1 form and at 800 °C by the appearance of about 10% of the equilibrium t–ZrO_2, a further reduction of the asymmetry parameter, and the change of movement of the vacancies from a slow to a fast diffusion. A possible interpretation of these experimental effects, which occur at temperatures between that of the smooth mass loss (TGA in oxygen) and those of the removal of the last $(OH)^-$ groups (DTA) and the oxygen gain (TGA), can be supported by the following hypothesis: (i) both the presence of initial structural oxygen vacancies due to the Y^{3+} cations and the progressive removal of the aquo, organic, and surface $(OH)^-$ groups favor, at the crystallization temperature, the predominance of a very defective tetragonal-like structure, the t_1 form; (ii) under the assumption that the smooth mass loss observed at 450 °C is the average result of a drastic mass loss (as observed in argon) and some oxygen absorption in order to overcome the resulting growing defect imbalance, a redistribution of the oxygen vacancies above this temperature causes a fraction of the tetragonal t_1 form to appear less distorted and the other fraction to give rise to the t_2 form; and (iii) the apparent oxygen incorporation at higher temperatures, likely forced by the disappearance of the last $(OH)^-$ residues, causes healing of some vacancies, so that a fraction of the t_1 form describes an even more symmetric EFG and the remaining fraction becomes the eightfold oxygen coordinated t–ZrO_2 phase. This new defect distribution favors a faster movement of the vacancies.

(e) At 1000 °C, concomitant with a relevant increase in the crystallite size (see Fig. 4), the appearance of about 20% of a somewhat distorted monoclinic phase[9] at the expense of the t_2 form was observed.

(f) The sudden cooling to RT (see qRT spectrum in Fig. 5), performed to test the thermal stability of the tetragonal structure, yielded some reversal in the distribution of the existing defects. As result, the amount of Zr^{4+} sites surrounded by near bound vacancies (t_1 form) increases at the expense of both the less defective t_2 form and the perfect t–ZrO_2, which disappears. In addition, a small amount of m–ZrO_2 remains, confirming the XRD results of Fig. 2 in that the presence of monoclinic zirconia upon cooling from high temperatures is constrained to the availability of oxygen.

(g) Subsequent measurements at 1100 (not shown in Fig. 6) and 1200 °C showed a hyperfine pattern similar to the one obtained from the previous gradual heating: the two interactions corresponding to the t_2 and t_1

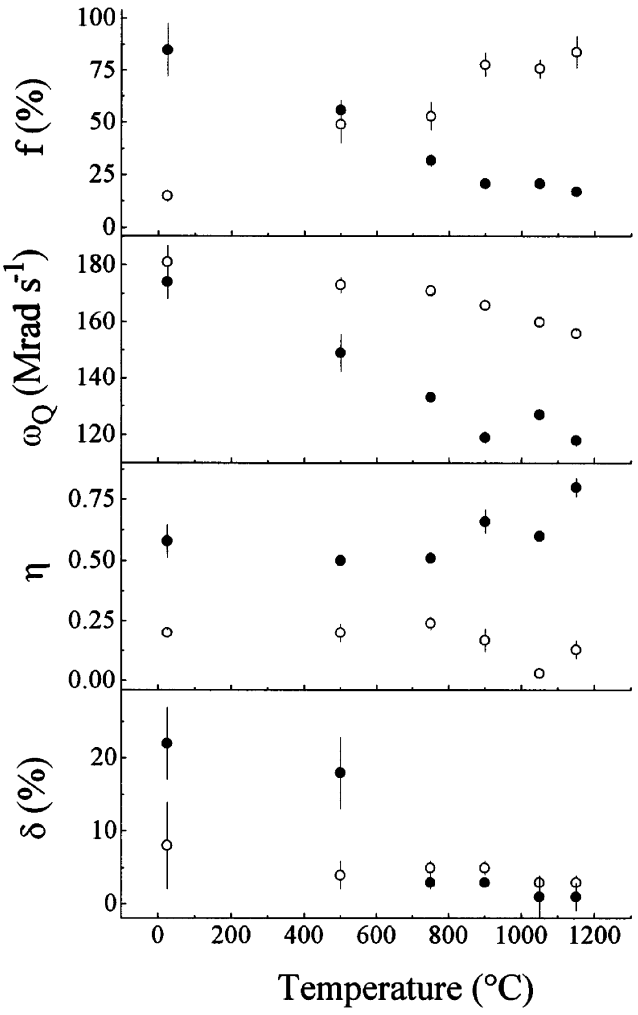

FIG. 7. Thermal evolution of the relative fractions and quadrupole parameters of the hyperfine interactions found for the coating. The symbols are the same as in Fig. 6.

forms in a high t_2/t_1 ratio and noticeable amounts of t–ZrO_2 and m–ZrO_2. The next experiment, performed again at 1000 °C, resulted in the complete vanishing of the equilibrium m– and t–ZrO_2 phases. This effect revealed the unstable nature of the m–ZrO_2 structure appearing before within the 1000–1200 °C temperature range. During subsequent measurements at decreasing temperatures down to 650 °C, a nearly constant t_2/t_1 ratio was observed, in agreement with the absence of any change in the DTA and TGA cooling curves within this thermal range.

(h) At 550 °C, on the other hand, both the decrease in the t_1 form population and increase in its η parameter precluded the next change. In fact, at 450 °C, m–ZrO_2 reappeared to continually increase at the expense of the t_2 form, once the t_1 form had vanished at 350 °C, and some irregularities in the η and δ parameters of the parent t_2 form could be observed. The $t_2 \rightarrow m$ transformation involved, leading to 95% of the m–ZrO_2 in the final

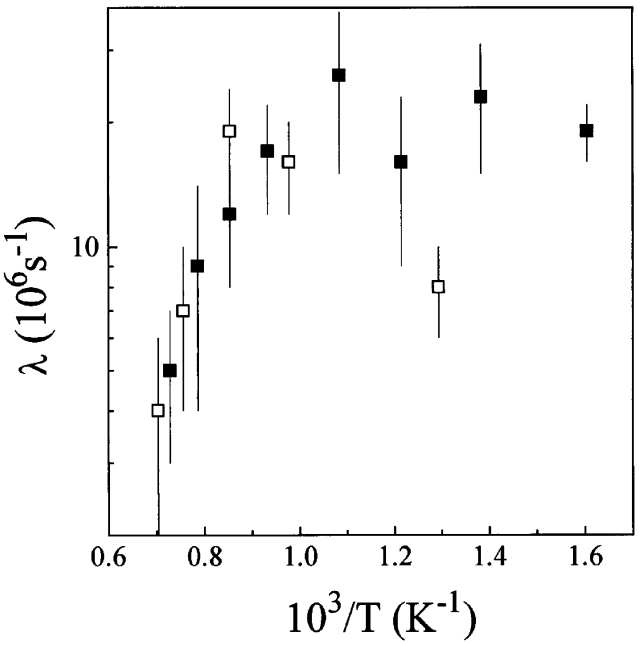

FIG. 8. Thermal behavior of the relaxation constant describing the two-regime diffusion of the oxygen vacancies, as seen by the Hf(Zr) probes at the t_2–tetragonal form. (■) Powder and (□) coating.

measurement at RT, is probably in correspondence with the wide endothermic peak in the DTA cooling curve. Reflecting that when the sample was suddenly cooled from 1000 °C (PAC experiment) or from 1060 °C (XRD in oxygen) to RT only small amounts of m–ZrO_2 were retained, an explanation for the discrepancy between this result and the predominant presence of m–ZrO_2 in the last PAC measurement can be postulated considering the two different aging thermal histories. As is known from the ZrO_2–Y_2O_3 equilibrium phase diagram,[19] 500 °C is a critical temperature for the stability of a tetragonal zirconia system of the present composition. Our PAC results seem to indicate that only if the grain had attained the proper size at the highest temperatures will the ceramic undergo its complete degradation when cooled gradually below the critical temperature.

Though few measurements could be performed due to the poor ^{181}Hf activity achieved in the thin film, this sample seemed to behave more simply than the powder, as can be seen from Fig. 7. In fact, (a) only the two interactions corresponding to the t_1 and t_2 forms were found over the RT–1150 °C thermal range investigated, the t_1 form transforming into t_2 with temperature. m–ZrO_2 was never observed, either at high temperatures near the equilibrium $m \rightarrow t$ transition temperature or upon cooling to RT in the final experiment; (b) from 800 °C on, the η parameter of the t_1 form increased, exhibiting a behavior opposite to that observed for the powder; and (c) cooling from 1150 °C to RT caused the already reported $t_2 \rightarrow t_1$ reverse transformation. At this point it seems worthwhile to recall the interpretation given

for the powder in that the oxygen income could be reflected in the reduction of the asymmetry parameter of the t_1 form and also in the final result of the appearance of t–ZrO_2 and m–ZrO_2 at the expense of both the t_1 and t_2 metastable tetragonal forms. In fact, according to this interpretation, the opposite effects of the increase in the axial asymmetry of the t_1 EFG and the absence of t–ZrO_2 and m–ZrO_2 observed for the coating above 750 °C (see Fig. 7) would correspond to increasingly defective, oxygen-deficient zirconium surroundings. This microscopic description seems to be an important point to take into account concerning the better stability of the coating as compared with the powder: in view of the present results, the stability of the tetragonal phase could be associated with the increase or at least maintenance of the t_1 EFG asymmetry and this maintenance, with some difficulty of the lattice to incorporate atmospheric oxygen, thus preserving the nonstoichiometry of stabilized tetragonal zirconia. A possible connection between the highly defective nature of the metastable t_1 form and some already known bulk conditions aiding the tetragonal phase stabilization, i.e., smaller grain size and the presence of residual lattice strains, deserves a special investigation.

Concerning the movement of oxygen vacancies, the $\lambda(T^{-1})$ function is plotted in Fig. 8. For both the coating and the powder a slow-fast two-regime behavior can be observed. The movements at temperatures lower than 800 °C correspond, according to the dynamic model assumed, to a slow diffusion for which an activation energy is hard to derive, as can be seen from the experimental points. At higher temperatures, in turn, the fast relaxation can be considered Arrhenius-like and an activation energy of 0.54 ± 0.14 eV could be drawn from the $\lambda(T^{-1})$ slope. This value, which resulted similarly to that determined by the authors for a commercial stabilized tetragonal zirconia,[14] is near half the values reported for cubic zirconias.[9,13]

IV. CONCLUSIONS

(1) The sol-gel derived ceramic under study crystallizes above 450 °C into the already known tetragonal t_1 and t_2 forms, the t_1 form being a highly defective microstructure. This microscopic description is in correspondence with a diffraction pattern indistinguishable from that of the equilibrium t–ZrO_2 phase and a crystallite size smaller than 20 nm. As temperature is raised, the lattice undergoes the $t_1 \rightarrow t_2$ transformation. According to previous literature, these results seem to be independent of the sample preparation method.

(2) Oxygen seems to play an important role respecting tetragonal zirconia stability. In the powder samples, oxygen absorption at moderate heating temperatures is concomitant with noticeable hyperfine changes reflecting the transition toward less defective structures which probably end at higher temperatures in a partial destabilization. The definitive degradation of the ceramic is accomplished through the t_2 form $\rightarrow$ m–ZrO_2 phase transformation, which occurred when cooling gradually in air below 500 °C, provided the grain had attained the proper size after long aging at high temperatures. The film, as compared with the powder, exhibits a better thermal stability.

(3) The fast diffusion of the oxygen vacancies is observed once the lattice has eliminated most of the synthesis-derived residues and is characterized by an activation energy of 0.54 ± 0.14 eV.

ACKNOWLEDGMENTS

Partial financial support from CONICET and CICPBA is gratefully acknowledged.

REFERENCES

1. A. H. Heuer, R. Chaim, and V. Lanteri, in *Advances in Ceramics,* edited by S. Sōmiya, N. Yamamoto, and H. Yanagida (The American Ceramic Society, Westerville, OH, 1988), Vol. 24a, p. 3.
2. H. Schubert and G. Petzow, in *Advances in Ceramics,* edited by S. Sōmiya, N. Yamamoto, and H. Yanagida (The American Ceramic Society, Westerville, OH, 1988), Vol. 24a, p. 21.
3. K. Tsukuma, K. Ueda, K. Matsushita, and M. Shimada, J. Am. Ceram. Soc. **68** (2), C-56 (1985).
4. S. Stecura, Am. Ceram. Bull. **56** (12), 1082 (1977).
5. B. E. Yoldas, J. Mater. Sci, **21**, 1080 (1986).
6. P. C. Rivas, J. A. Martínez, M. C. Caracoche, A. R. López García, L. C. Klein, and R. S. Pavlik, Jr., J. Am. Ceram. Soc. **78** (5), 1329 (1995).
7. R. Caruso, N. Pellegri, O. de Sanctis, M. C. Caracoche, and P. C. Rivas, J. Sol-Gel Sci. Technol. **3**, 241 (1994).
8. P. C. Rivas, M. C. Caracoche, J. A. Martínez, A. M. Rodríguez, R. Caruso, N. Pellegri, and O. de Sanctis, J. Mater. Res. **12**, 493 (1997).
9. H. Jaeger, Ph.D. Thesis, Oregon State University, 1987.
10. H. Frauenfelder and R. M. Steffen, in *Alpha, Beta and Gamma Spectroscopies,* edited by K. Siegbahn (North-Holland, Amsterdam, The Netherlands, 1965), Chap. XIX.
11. H. Jaeger, J. A. Gardner, J. C. Haygarth, and R. L. Rasera, J. Am. Ceram. Soc. **69** (6), 458 (1986).
12. J. A. Gardner, H. Jaeger, H. T. Su, W. H. Warner, and J. C. Haygarth, Physica B**150**, 223 (1988).
13. P. C. Rivas, M. C. Caracoche, A. F. Pasquevich, J. A. Martínez, A. M. Rodríguez, A. R. López García, and S. Mintzer, J. Am. Ceram. Soc. **79** (4), 831 (1996).
14. A. J. Marshall and C. F. Meares, J. Chem. Phys. **56** (3), 1226 (1972).
15. A. Caneiro, P. Baudaz, J. Fouletier, and J. P. Abriata, Rev. Sci. Instrum. **53**, 1072 (1982).
16. H. P. Klug and L. E. Alexander, *X-Ray Diffraction Procedures for Polycrystalline and Amorphous Materials,* 2nd ed. (John Wiley, New York, 1974), Chap. 9.
17. C. Barrera-Solano, C. Jiménez Solis, N. dela Rosa-Fox, and L. Esquivias, J. Sol-Gel Sci. Technol. **2**, 347 (1994).
18. Ph. Colomban and E. Bruneton, J. Non-Cryst. Solids **147 & 148**, 201 (1992).
19. R. Ruh, R. S. Mazdiyasni, P. Valentine, and H. Bielstein, J. Am. Ceram. Soc. **67**, C-190 (1984).